

Probing Balitsky-Fadin-Kuraev-Lipatov Dynamics in the Dijet Cross Section at Large Rapidity Intervals in $p\bar{p}$ Collisions at $\sqrt{s} = 1800$ and 630 GeV

B. Abbott,⁴⁶ M. Abolins,⁴³ V. Abramov,¹⁹ B. S. Acharya,¹³ D. L. Adams,⁵³ M. Adams,³⁰ V. Akimov,¹⁷ G. A. Alves,² N. Amos,⁴² E. W. Anderson,³⁵ M. M. Baarmand,⁴⁸ V. V. Babintsev,¹⁹ L. Babukhadia,⁴⁸ A. Baden,³⁹ B. Baldin,²⁹ S. Banerjee,¹³ J. Bantly,⁵² E. Barberis,²² P. Baringer,³⁶ J. F. Bartlett,²⁹ U. Bassler,⁹ A. Bean,³⁶ A. Belyaev,¹⁸ S. B. Beri,¹¹ G. Bernardi,⁹ I. Bertram,²⁰ V. A. Bezzubov,¹⁹ P. C. Bhat,²⁹ V. Bhatnagar,¹¹ M. Bhattacharjee,⁴⁸ G. Blazey,³¹ S. Blessing,²⁷ A. Boehnlein,²⁹ N. I. Bojko,¹⁹ F. Borchering,²⁹ A. Brandt,⁵³ R. Breedon,²³ G. Briskin,⁵² R. Brock,⁴³ G. Brooijmans,²⁹ A. Bross,²⁹ D. Buchholz,³² V. Buescher,⁴⁷ V. S. Burtovoi,¹⁹ J. M. Butler,⁴⁰ W. Carvalho,³ D. Casey,⁴³ Z. Casilum,⁴⁸ H. Castilla-Valdez,¹⁵ D. Chakraborty,⁴⁸ K. M. Chan,⁴⁷ S. V. Chekulaev,¹⁹ W. Chen,⁴⁸ D. K. Cho,⁴⁷ S. Choi,²⁶ S. Chopra,²⁷ B. C. Choudhary,²⁶ J. H. Christenson,²⁹ M. Chung,³⁰ D. Claes,⁴⁴ A. R. Clark,²² W. G. Cobau,³⁹ J. Cochran,²⁶ L. Coney,³⁴ B. Connolly,²⁷ W. E. Cooper,²⁹ D. Coppage,³⁶ D. Cullen-Vidal,⁵² M. A. C. Cummings,³¹ D. Cutts,⁵² O. I. Dahl,²² K. Davis,²¹ K. De,⁵³ K. Del Signore,⁴² M. Demarteau,²⁹ D. Denisov,²⁹ S. P. Denisov,¹⁹ H. T. Diehl,²⁹ M. Diesburg,²⁹ G. Di Loreto,⁴³ P. Draper,⁵³ Y. Ducros,¹⁰ L. V. Dudko,¹⁸ S. R. Dugad,¹³ A. Dyshkant,¹⁹ D. Edmunds,⁴³ J. Ellison,²⁶ V. D. Elvira,²⁹ R. Engelmann,⁴⁸ S. Eno,³⁹ G. Eppley,⁵⁵ P. Ermolov,¹⁸ O. V. Eroshin,¹⁹ J. Estrada,⁴⁷ H. Evans,⁴⁵ V. N. Evdokimov,¹⁹ T. Fahland,²⁵ S. Feher,²⁹ D. Fein,²¹ T. Ferbel,⁴⁷ H. E. Fisk,²⁹ Y. Fisyak,⁴⁹ E. Flattum,²⁹ F. Fleuret,²² M. Fortner,³¹ K. C. Frame,⁴³ S. Fuess,²⁹ E. Gallas,²⁹ A. N. Galyaev,¹⁹ P. Gartung,²⁶ V. Gavrilov,¹⁷ R. J. Genik II,²⁰ K. Genser,²⁹ C. E. Gerber,²⁹ Y. Gershtein,⁵² B. Gibbard,⁴⁹ R. Gilmartin,²⁷ G. Ginther,⁴⁷ B. Gobbi,³² B. Gómez,⁵ G. Gómez,³⁹ P. I. Goncharov,¹⁹ J. L. González Solís,¹⁵ H. Gordon,⁴⁹ L. T. Goss,⁵⁴ K. Gounder,²⁶ A. Goussiou,⁴⁸ N. Graf,⁴⁹ P. D. Grannis,⁴⁸ J. A. Green,³⁵ H. Greenlee,²⁹ S. Grinstein,¹ P. Grudberg,²² S. Grünendahl,²⁹ G. Guglielmo,⁵¹ A. Gupta,¹³ S. N. Gurzhiev,¹⁹ G. Gutierrez,²⁹ P. Gutierrez,⁵¹ N. J. Hadley,³⁹ H. Haggerty,²⁹ S. Hagopian,²⁷ V. Hagopian,²⁷ K. S. Hahn,⁴⁷ R. E. Hall,²⁴ P. Hanlet,⁴¹ S. Hansen,²⁹ J. M. Hauptman,³⁵ C. Hays,⁴⁵ C. Hebert,³⁶ D. Hedin,³¹ A. P. Heinson,²⁶ U. Heintz,⁴⁰ T. Heuring,²⁷ R. Hirosky,³⁰ J. D. Hobbs,⁴⁸ B. Hoeneisen,⁶ J. S. Hoftun,⁵² A. S. Ito,²⁹ S. A. Jerger,⁴³ R. Jesik,³³ T. Joffe-Minor,³² K. Johns,²¹ M. Johnson,²⁹ A. Jonckheere,²⁹ M. Jones,²⁸ H. Jöstlein,²⁹ S. Y. Jun,³² A. Juste,²⁹ S. Kahn,⁴⁹ E. Kajfasz,⁸ D. Karmanov,¹⁸ D. Karmgard,³⁴ R. Kehoe,³⁴ S. K. Kim,¹⁴ B. Klima,²⁹ C. Klopfenstein,²³ B. Knuteson,²² W. Ko,²³ J. M. Kohli,¹¹ A. V. Kostritskiy,¹⁹ J. Kotcher,⁴⁹ A. V. Kotwal,⁴⁵ A. V. Kozelov,¹⁹ E. A. Kozlovsky,¹⁹ J. Krane,³⁵ M. R. Krishnaswamy,¹³ S. Krzywdzinski,²⁹ M. Kubantsev,³⁷ S. Kuleshov,¹⁷ Y. Kulik,⁴⁸ S. Kunori,³⁹ G. Landsberg,⁵² A. Leflat,¹⁸ F. Lehner,²⁹ J. Li,⁵³ Q. Z. Li,²⁹ J. G. R. Lima,³ D. Lincoln,²⁹ S. L. Linn,²⁷ J. Linnemann,⁴³ R. Lipton,²⁹ J. G. Lu,⁴ A. Lucotte,⁴⁸ L. Lueking,²⁹ C. Lundstedt,⁴⁴ A. K. A. Maciel,³¹ R. J. Madaras,²² V. Manankov,¹⁸ S. Mani,²³ H. S. Mao,⁴ R. Markeloff,³¹ T. Marshall,³³ M. I. Martin,²⁹ R. D. Martin,³⁰ K. M. Mauritz,³⁵ B. May,³² A. A. Mayorov,³³ R. McCarthy,⁴⁸ J. McDonald,²⁷ T. McKibben,³⁰ T. McMahon,⁵⁰ H. L. Melanson,²⁹ M. Merkin,¹⁸ K. W. Merritt,²⁹ C. Miao,⁵² H. Miettinen,⁵⁵ D. Mihalcea,⁵¹ A. Mincer,⁴⁶ C. S. Mishra,²⁹ N. Mokhov,²⁹ N. K. Mondal,¹³ H. E. Montgomery,²⁹ M. Mostafa,¹ H. da Motta,² E. Nagy,⁸ F. Nang,²¹ M. Narain,⁴⁰ V. S. Narasimham,¹³ H. A. Neal,⁴² J. P. Negret,⁵ S. Negroni,⁸ D. Norman,⁵⁴ L. Oesch,⁴² V. Oguri,³ B. Olivier,⁹ N. Oshima,²⁹ P. Padley,⁵⁵ L. J. Pan,³² A. Para,²⁹ N. Parashar,⁴¹ R. Partridge,⁵² N. Parua,⁷ M. Paterno,⁴⁷ A. Patwa,⁴⁸ B. Pawlik,¹⁶ J. Perkins,⁵³ M. Peters,²⁸ R. Piegai,¹ H. Piekarczyk,²⁷ B. G. Pope,⁴³ E. Popkov,³⁴ H. B. Prosper,²⁷ S. Protopopescu,⁴⁹ J. Qian,⁴² P. Z. Quintas,²⁹ R. Raja,²⁹ S. Rajagopalan,⁴⁹ N. W. Reay,³⁷ S. Reucroft,⁴¹ M. Rijssenbeek,⁴⁸ T. Rockwell,⁴³ M. Roco,²⁹ P. Rubinov,³² R. Ruchti,³⁴ J. Rutherford,²¹ A. Santoro,² L. Sawyer,³⁸ R. D. Schamberger,⁴⁸ H. Schellman,³² A. Schwartzman,¹ J. Sculli,⁴⁶ N. Sen,⁵⁵ E. Shabalina,¹⁸ H. C. Shankar,¹³ R. K. Shivpuri,¹² D. Shpakov,⁴⁸ M. Shupe,²¹ R. A. Sidwell,³⁷ H. Singh,²⁶ J. B. Singh,¹¹ V. Sirotenko,³¹ P. Slattery,⁴⁷ E. Smith,⁵¹ R. P. Smith,²⁹ R. Snihur,³² G. R. Snow,⁴⁴ J. Snow,⁵⁰ S. Snyder,⁴⁹ J. Solomon,³⁰ X. F. Song,⁴ V. Sorín,¹ M. Sosebee,⁵³ N. Sotnikova,¹⁸ M. Souza,² N. R. Stanton,³⁷ G. Steinbrück,⁴⁵ R. W. Stephens,⁵³ M. L. Stevenson,²² F. Stichelbaut,⁴⁹ D. Stoker,²⁵ V. Stolin,¹⁷ D. A. Stoyanova,¹⁹ M. Strauss,⁵¹ K. Streets,⁴⁶ M. Strovink,²² L. Stutte,²⁹ A. Sznajder,³ J. Tarazi,²⁵ W. Taylor,⁴⁸ S. Tentindo-Repond,²⁷ T. L. T. Thomas,³² J. Thompson,³⁹ D. Toback,³⁹ T. G. Trippe,²² A. S. Turcot,⁴² P. M. Tuts,⁴⁵ P. van Gemmeren,²⁹ V. Vaniev,¹⁹ N. Varelas,³⁰ A. A. Volkov,¹⁹ A. P. Vorobiev,¹⁹ H. D. Wahl,²⁷ H. Wang,³² J. Warchol,³⁴ G. Watts,⁵⁶ M. Wayne,³⁴ H. Weerts,⁴³ A. White,⁵³ J. T. White,⁵⁴ D. Whiteson,²² J. A. Wightman,³⁵ S. Willis,³¹ S. J. Wimpenny,²⁶ J. V. D. Wirjawan,⁵⁴ J. Womersley,²⁹ D. R. Wood,⁴¹ R. Yamada,²⁹ P. Yamin,⁴⁹ T. Yasuda,²⁹ K. Yip,²⁹ S. Youssef,²⁷ J. Yu,²⁹ Z. Yu,³² M. Zanabria,⁵ H. Zheng,³⁴ Z. Zhou,³⁵ Z. H. Zhu,⁴⁷ M. Zielinski,⁴⁷ D. Zieminska,³³ A. Zieminski,³³ V. Zutshi,⁴⁷ E. G. Zverev,¹⁸ and A. Zylberstein¹⁰

(D0 Collaboration)

- ¹Universidad de Buenos Aires, Buenos Aires, Argentina
²LAFEX, Centro Brasileiro de Pesquisas Fisicas, Rio de Janeiro, Brazil
³Universidade do Estado do Rio de Janeiro, Rio de Janeiro, Brazil
⁴Institute of High Energy Physics, Beijing, People's Republic of China
⁵Universidad de los Andes, Bogotá, Colombia
⁶Universidad San Francisco de Quito, Quito, Ecuador
⁷Institut des Sciences Nucléaires, IN2P3-CNRS, Université de Grenoble I, Grenoble, France
⁸CPPM, IN2P3-CNRS, Université de la Méditerranée, Marseille, France
⁹LPNHE, Universités Paris VI and VII, IN2P3-CNRS, Paris, France
¹⁰DAPNIA/Service de Physique des Particules, CEA, Saclay, France
¹¹Panjab University, Chandigarh, India
¹²Delhi University, Delhi, India
¹³Tata Institute of Fundamental Research, Mumbai, India
¹⁴Seoul National University, Seoul, Korea
¹⁵CINVESTAV, Mexico City, Mexico
¹⁶Institute of Nuclear Physics, Kraków, Poland
¹⁷Institute for Theoretical and Experimental Physics, Moscow, Russia
¹⁸Moscow State University, Moscow, Russia
¹⁹Institute for High Energy Physics, Protvino, Russia
²⁰Lancaster University, Lancaster, United Kingdom
²¹University of Arizona, Tucson, Arizona 85721
²²Lawrence Berkeley National Laboratory and University of California, Berkeley, California 94720
²³University of California, Davis, California 95616
²⁴California State University, Fresno, California 93740
²⁵University of California, Irvine, California 92697
²⁶University of California, Riverside, California 92521
²⁷Florida State University, Tallahassee, Florida 32306
²⁸University of Hawaii, Honolulu, Hawaii 96822
²⁹Fermi National Accelerator Laboratory, Batavia, Illinois 60510
³⁰University of Illinois at Chicago, Chicago, Illinois 60607
³¹Northern Illinois University, DeKalb, Illinois 60115
³²Northwestern University, Evanston, Illinois 60208
³³Indiana University, Bloomington, Indiana 47405
³⁴University of Notre Dame, Notre Dame, Indiana 46556
³⁵Iowa State University, Ames, Iowa 50011
³⁶University of Kansas, Lawrence, Kansas 66045
³⁷Kansas State University, Manhattan, Kansas 66506
³⁸Louisiana Tech University, Ruston, Louisiana 71272
³⁹University of Maryland, College Park, Maryland 20742
⁴⁰Boston University, Boston, Massachusetts 02215
⁴¹Northeastern University, Boston, Massachusetts 02115
⁴²University of Michigan, Ann Arbor, Michigan 48109
⁴³Michigan State University, East Lansing, Michigan 48824
⁴⁴University of Nebraska, Lincoln, Nebraska 68588
⁴⁵Columbia University, New York, New York 10027
⁴⁶New York University, New York, New York 10003
⁴⁷University of Rochester, Rochester, New York 14627
⁴⁸State University of New York, Stony Brook, New York 11794
⁴⁹Brookhaven National Laboratory, Upton, New York 11973
⁵⁰Langston University, Langston, Oklahoma 73050
⁵¹University of Oklahoma, Norman, Oklahoma 73019
⁵²Brown University, Providence, Rhode Island 02912
⁵³University of Texas, Arlington, Texas 76019
⁵⁴Texas A&M University, College Station, Texas 77843
⁵⁵Rice University, Houston, Texas 77005
⁵⁶University of Washington, Seattle, Washington 98195

(Received 15 December 1999)

Inclusive dijet production at large pseudorapidity intervals ($\Delta\eta$) between the two jets has been suggested as a regime for observing Balitsky-Fadin-Kuraev-Lipatov (BFKL) dynamics. We have measured the dijet cross section for large $\Delta\eta$ in $p\bar{p}$ collisions at $\sqrt{s} = 1800$ and 630 GeV using the D0

detector. The partonic cross section increases strongly with the size of $\Delta\eta$. The observed growth is even stronger than expected on the basis of BFKL resummation in the leading logarithmic approximation. The growth of the partonic cross section can be accommodated with an effective BFKL intercept of $\alpha_{\text{BFKL}}(20 \text{ GeV}) = 1.65 \pm 0.07$.

PACS numbers: 13.87.-a, 12.38.-t

Jet production in the high-energy limit of quantum chromodynamics (QCD), as defined by center-of-mass (c.m.) energies (\sqrt{s}) much larger than the momentum transfers (Q), presents a very interesting and yet little explored area. In this kinematic region, the significantly different energy scales of the process lead to calculated jet cross sections characterized by the appearance of large logarithms $\ln(s/Q^2)$, which must be summed to all orders in α_s . This summation is accomplished through the Balitsky-Fadin-Kuraev-Lipatov (BFKL) [1] equation, which involves a spacelike chain of an infinite number of gluon emissions. The gluons have similar transverse momenta, but they are strongly ordered in their pseudorapidities or, equivalently, in their longitudinal momentum fractions x_i . Thus, the BFKL equation effectively describes the evolution in x (growth with $1/x$) of the gluon momentum distribution in the proton.

Attempts to isolate and probe the BFKL evolution in the low- x region in ep collisions at HERA, by measuring the forward jet and particle cross sections [2], have led to ambiguous results. (At HERA, forward denotes the region away from the current jet and towards the proton remnant.) In $p\bar{p}$ collisions, the azimuthal decorrelation as a function of the pseudorapidity interval, $\Delta\eta$, in dijet systems has been studied [3]. (Here, $\eta = -\ln[\tan(\theta/2)]$, where θ is the polar angle of the jet relative to the proton beam.) It has been argued [4], however, that the azimuthal angle distribution is not an inclusive enough quantity for the cancellation between the real and virtual soft gluons that accompany dijet production; thus, such a distribution cannot be used as a probe of the BFKL equation.

Inclusive dijet production at large pseudorapidity intervals in high-energy $p\bar{p}$ collisions, on the other hand, provides an excellent testing ground for BFKL dynamics. We present a measurement of the dijet cross section at large $\Delta\eta$ using the D0 detector at the Fermilab Tevatron collider. We reconstruct the event kinematics using the most forward/backward jets, and measure the cross section as a function of x_1 , x_2 , and Q^2 . The longitudinal momentum fractions of the proton and antiproton, x_1 and x_2 , carried by the two interacting partons are defined as

$$x_{1,2} = \frac{2E_{T_{1,2}}}{\sqrt{s}} e^{\pm\bar{\eta}} \cosh(\Delta\eta/2), \quad (1)$$

where $E_{T_1}(E_{T_2})$ and $\eta_1(\eta_2)$ are the transverse energy and pseudorapidity of the most forward(backward) jet, $\Delta\eta = \eta_1 - \eta_2 \geq 0$, and $\bar{\eta} = (\eta_1 + \eta_2)/2$. The momentum transfer during the hard scattering is defined as

$$Q = \sqrt{E_{T_1}E_{T_2}}. \quad (2)$$

The total dijet cross section, σ , can be factorized into the partonic cross section, $\hat{\sigma}$, and the parton distribution functions (PDF), $P(x_{1,2}, Q^2)$, in the proton and antiproton: $\sigma = x_1 P(x_1, Q^2) x_2 P(x_2, Q^2) \hat{\sigma}$. The partonic c.m. energy, $\sqrt{\hat{s}}$, equals $\sqrt{x_1 x_2 s}$. For sufficiently large values of x_1 and x_2 , any large $\alpha_s \ln(s/Q^2)$ terms in σ correspond to large $\alpha_s \ln(\hat{s}/Q^2)$, which are of the order of $\alpha_s \Delta\eta$, and factorize in $\hat{\sigma}$. Using the BFKL prescription to sum the leading logarithmic terms $\alpha_s \ln(\hat{s}/Q^2)$ to all orders in α_s , results in an exponential rise of $\hat{\sigma}$ with $\Delta\eta$ [5]:

$$\hat{\sigma}_{\text{BFKL}} \propto \frac{1}{Q^2} \cdot \frac{e^{(\alpha_{\text{BFKL}}-1)\Delta\eta}}{\sqrt{\alpha_s \Delta\eta}}, \quad (3)$$

where α_{BFKL} is the BFKL intercept that governs the strength of the growth of the gluon distribution at small x . In the leading logarithmic approximation (LLA), α_{BFKL} is given by [1]:

$$\alpha_{\text{BFKL}} - 1 = \frac{\alpha_s(Q) 12 \ln 2}{\pi}. \quad (4)$$

The predicted rise of the partonic cross section with $\Delta\eta$ is difficult to observe experimentally due to the dependence of the total cross section on the PDF. To overcome this difficulty, we measure the cross section at two c.m. energies, $\sqrt{s_A} = 1800 \text{ GeV}$ and $\sqrt{s_B} = 630 \text{ GeV}$, and take their ratio for the same values of x_1 , x_2 , and Q^2 . This eliminates the dependence on the PDF, and reduces the ratio to that of the partonic cross sections. The latter is purely a function of the $\Delta\eta$ values:

$$R \equiv \frac{\sigma(\sqrt{s_A})}{\sigma(\sqrt{s_B})} = \frac{\hat{\sigma}(\Delta\eta_A)}{\hat{\sigma}(\Delta\eta_B)} = \frac{e^{(\alpha_{\text{BFKL}}-1)(\Delta\eta_A - \Delta\eta_B)}}{\sqrt{\Delta\eta_A/\Delta\eta_B}}. \quad (5)$$

Thus, varying \sqrt{s} , while keeping x_1 , x_2 , and Q^2 fixed, is equivalent to varying $\Delta\eta$, which directly probes the BFKL dynamics. In addition, measurement of the ratio leads to cancellation of certain experimental uncertainties, and enables an experimental extraction of α_{BFKL} .

In the D0 [6] detector, jets are identified using the uranium/liquid-argon calorimeters. These cover the range of $|\eta| \leq 4.1$, and are segmented into towers of $\Delta\eta \times \Delta\phi = 0.1 \times 0.1$ (ϕ is the azimuthal angle).

The data samples for this analysis were collected during the 1995–1996 Tevatron Collider run. Events were selected online by a three-level trigger system culminating in the software trigger requirement of a jet candidate with $E_T > 12 \text{ GeV}$. The trigger was 85% efficient for jets with $E_T = 20 \text{ GeV}$, and fully efficient for jets with $E_T > 30 \text{ GeV}$. The integrated luminosity of the trigger was 0.7 nb^{-1} for the $\sqrt{s} = 1800 \text{ GeV}$ sample, and 31.8 nb^{-1} for the $\sqrt{s} = 630 \text{ GeV}$ sample [7].

Jets were reconstructed offline using an iterative fixed-cone algorithm with a cone radius of $\mathcal{R} = 0.7$ in (η, ϕ) space [8]. The pseudorapidity of each jet was corrected for small reconstruction and jet algorithm biases. The transverse energy of each jet was corrected in three stages: (i) Energy originating from spectator parton interactions, additional $p\bar{p}$ interactions, noise from uranium decay, and residual energy from previous $p\bar{p}$ interactions was subtracted on average from the measured jet energy [9]; (ii) The jet energy was corrected for the hadronic response of the calorimeter [9]; (iii) The fraction of the particle energy that showered outside of the jet reconstruction cone was recovered, and the fraction of the energy reconstructed within the cone that did not belong to the original particle was subtracted [10]. The average correction for jets of $E_T = 20$ GeV and $|\eta| = 2.5$ is $(22.8 \pm 4.8)\%$ at $\sqrt{s} = 1800$ GeV; for jets of the same E_T and $|\eta| = 1.2$ the correction is $(14.5 \pm 4.0)\%$ at 630 GeV.

The event vertex was required to lie within 50 cm of the detector center; 93% (86)% of the events at 1800(630) GeV satisfied this requirement. To remove cosmic ray background, the imbalance in the transverse momentum of the event was required to be less than 70% of the leading jet E_T ; more than 98% of the events at each c.m. energy satisfied this requirement. To ensure good jet reconstruction efficiency and jet energy calibration, jets were selected with $E_T > 20$ GeV and $|\eta| < 3$. Backgrounds from isolated noisy calorimeter cells, accelerator beam losses, and electromagnetic clusters that mimic jets were eliminated by applying a series of jet quality criteria; 97% of the jets survived this final selection.

The selected jets of each event were ordered in pseudorapidity. A minimum pseudorapidity interval of $\Delta\eta > 2$ was required between the most forward and most backward jet. In the final samples, the most forward and most backward jets were found to have approximately the same E_T . The values of x_1 , x_2 , and Q^2 were calculated from Eqs. (1) and (2). Most of the data at $\sqrt{s} = 1800$ GeV are within $0.01 < x_{1,2} < 0.30$, and at 630 GeV, within $0.03 < x_{1,2} < 0.60$. The region of maximum overlap, $0.06 < x_{1,2} < 0.30$, was divided into six equal bins of x_1 and x_2 . Because of limited statistics, only one bin in Q^2 was used: $400 < Q^2 < 1000$ GeV². The dijet cross section, corrected for trigger, event, and jet selection inefficiencies, was computed in each (x_1, x_2, Q^2) bin.

The dijet cross section at low (x_1, x_2) is affected by the acceptance of the $E_T > 20$ GeV and $\Delta\eta > 2$ requirements. To avoid this bias, we require $x_1 \cdot x_2 > 0.01$. Similarly, the cross section at high (x_1, x_2) is biased by the $|\eta| < 3$ requirement, so that we require $x_{1,2} < 0.22$. A total of ten (x_1, x_2) bins satisfy both requirements.

Multiple $p\bar{p}$ interactions during the same beam crossing, which, in principle, could distort the topology of the event and bias the cross section, were infrequent for the low instantaneous luminosity [$\mathcal{L} < 10^{30}(2 \times 10^{30})$ cm⁻² s⁻¹ at $\sqrt{s} = 1800(630)$ GeV] data used in this analysis. Nevertheless, any possible luminosity

effects on the dijet cross section were evaluated by measuring the cross section at 630 GeV from lower- and higher-luminosity subsamples. No significant difference was observed between the two measurements.

The dijet cross section is distorted by jet energy resolution. The resolution was measured as a function of jet pseudorapidity and E_T , by balancing E_T in events with only two jets back-to-back in ϕ . For jets of $E_T = 20$ GeV, the fractional E_T resolution is 27%(14%) at $|\eta| = 1.2(2.5)$ and $\sqrt{s} = 1800$ GeV (measured from the jet data collected during the 1994–1995 92 pb⁻¹ Tevatron run). At $\sqrt{s} = 630$ GeV, limited statistics prohibited the measurement of the resolutions in the whole E_T and η spectrum. In the regions where the measurement was possible, the resolutions at 630 GeV were found to be smaller than the resolutions at 1800 GeV by $\sim 1\%$.

The distortion of the cross section was corrected using the HERWIG [11] Monte Carlo (MC) event generator, convoluted with the CTEQ4M [12] PDF. In the MC events, the jet transverse energies were smeared using the resolutions extracted from the 1800 GeV data. The $E_T > 20$ GeV, $|\eta| < 3$, and $\Delta\eta > 2$ requirements were applied separately to the original fully fragmented (particle-level) jets and to the E_T -smeared jets. Particle-level and smeared dijet cross sections were calculated in the same (x_1, x_2, Q^2) bins as in the data. Apart from normalization differences, the smeared HERWIG cross section at both c.m. energies exhibits the same dependence on $x_{1,2}$ as the data. The ratio of the particle-level to the smeared MC cross section in each bin was used as an unsmearing factor to correct the data cross section for the jet energy resolution effects. The unsmearing correction for the dijet cross section is typically of the order of 10% at both c.m. energies, whereas the unsmearing correction for the ratio of the cross sections amounts to only 6%. The difference between the measured resolutions at the two c.m. energies was accounted for in the systematic uncertainties. The unsmearing method was verified by using a smeared MC sample generated with ISAJET [13], and comparing the ISAJET particle-level cross section to that obtained using our unsmearing procedure based on HERWIG.

The dijet cross sections for $\Delta\eta > 2$ at $\sqrt{s} = 1800$ and 630 GeV in the selected (x_1, x_2) bins are shown in Table I. In each bin, the average values of x_1 , x_2 , and Q^2 are in good agreement, within the precision of our measurement, between the two c.m. energies. This ensures the cancellation of the PDF in the ratio of the cross sections. Also shown in the Table are the values for the BFKL intercept, α_{BFKL} , extracted from the cross sections and the average pseudorapidity intervals at 1800 and 630 GeV in each (x_1, x_2) bin, using Eq. (5).

The mean value of the ratios of the cross sections in the ten bins is equal to $\langle R \rangle \equiv \langle \sigma_{1800}/\sigma_{630} \rangle = 2.8 \pm 0.3(\text{stat})$. The mean value of α_{BFKL} is equal to $1.65 \pm 0.05(\text{stat})$. The mean pseudorapidity interval, $\langle \Delta\eta \rangle$, in the selected bins is equal to 4.6 units at 1800 GeV and 2.4 units at 630 GeV.

TABLE I. The dijet cross sections for $\Delta\eta > 2$ at $\sqrt{s} = 1800$ and 630 GeV and the extracted value of the BFKL intercept in each of the ten (x_1, x_2) bins. The minimum jet E_T is 20 GeV. The uncertainties are statistical.

x_1 range	x_2 range	σ_{1800} (nb)	σ_{630} (nb)	α_{BFKL}
0.06–0.10	0.18–0.22	28.1 ± 6.9	8.4 ± 0.9	1.74 ± 0.13
0.10–0.14	0.14–0.18	40.1 ± 9.5	8.8 ± 0.9	1.83 ± 0.11
...	0.18–0.22	$3.6 \pm_{-2.3}^{+4.1}$	5.4 ± 0.6	$0.96 \pm_{-0.28}^{+0.49}$
0.14–0.18	0.10–0.14	27.9 ± 7.3	8.4 ± 0.8	1.71 ± 0.13
...	0.14–0.18	$10.4 \pm_{-5.0}^{+6.1}$	5.0 ± 0.6	$1.50 \pm_{-0.24}^{+0.29}$
...	0.18–0.22	$5.6 \pm_{-3.8}^{+4.5}$	2.9 ± 0.5	$1.44 \pm_{-0.32}^{+0.38}$
0.18–0.22	0.06–0.10	26.3 ± 6.6	8.6 ± 0.9	1.71 ± 0.14
...	0.10–0.14	$12.5 \pm_{-5.4}^{+6.3}$	6.3 ± 0.7	$1.46 \pm_{-0.21}^{+0.24}$
...	0.14–0.18	$6.8 \pm_{-3.2}^{+5.0}$	3.1 ± 0.4	$1.50 \pm_{-0.23}^{+0.34}$
...	0.18–0.22	$2.4 \pm_{-1.7}^{+2.8}$	1.7 ± 0.3	$1.28 \pm_{-0.37}^{+0.60}$

The largest sources of systematic uncertainties on the ratio of the cross sections and the BFKL intercept are the jet energy scale (yielding an 8% uncertainty on the ratio and 2% on the intercept) and the jet energy resolutions (7% on the ratio and 2% on the intercept). The individual components of these were evaluated for correlations between the two data samples. Additional sources of systematic uncertainties on the ratio and the intercept include the choice of the input PDF in the Monte Carlo used for unsmearing (1% on the ratio, negligible on the intercept), and the uncertainty in the normalization of the luminosity (2% on the ratio and 1% on the intercept). The total systematic uncertainty amounts to 11% on the ratio of the cross sections and 3% on the BFKL intercept, yielding the final results:

$$\langle R \rangle = 2.8 \pm 0.3(\text{stat}) \pm 0.3(\text{syst}) = 2.8 \pm 0.4,$$

$$\begin{aligned} \langle \alpha_{\text{BFKL}} \rangle &= 1.65 \pm 0.05(\text{stat}) \pm 0.05(\text{syst}) \\ &= 1.65 \pm 0.07. \end{aligned}$$

Hence, for the same values of x_1 , x_2 , and Q^2 , the dijet cross section at large $\Delta\eta$ increases by almost a factor of 3 between the two c.m. energies, corresponding to the increase of $\langle \Delta\eta \rangle$ from 2.4 to 4.6 units.

Several theoretical predictions can be compared to our measurement. Leading order QCD predicts the ratio of the cross sections to fall asymptotically toward unity with increasing $\Delta\eta$. For the $\Delta\eta$ values relevant to this analysis, the predicted ratio is $R_{\text{LO}} = 1.2$ [14].

The HERWIG MC provides an alternative prediction. It calculates the exact $2 \rightarrow 2$ subprocess, including initial and final state radiation and angular ordering of the emitted partons. Using the same (x_1, x_2, Q^2) bins as in the data yields $R_{\text{HERWIG}} = 1.6 \pm 0.1(\text{stat})$.

The LLA BFKL intercept according to Eq. (4) for $\alpha_s(20 \text{ GeV}) = 0.17$ [14] is $\alpha_{\text{BFKL,LLA}} = 1.45$. For $\Delta\eta_{1800} = 4.6$ and $\Delta\eta_{630} = 2.4$, Eq. (5) yields $R_{\text{BFKL,LLA}} = 1.9$. It should be noted, however, that the leading log approximation may be too simplistic, and

that exact quantitative predictions including the next-to-leading logarithmic [15] corrections to the BFKL kernel are not as yet available.

It is evident that the growth of the dijet cross section with $\Delta\eta$ (from $\langle \Delta\eta \rangle = 2.4$ to 4.6) is stronger in the data than in the theoretical models we considered. The measured ratio is higher as listed: by 4 standard deviations than the LO prediction, by 3 deviations than the HERWIG prediction, and by 2.3 deviations than the LLA BFKL prediction.

It should be noted that the $x_{1,2}$ definitions of Eq. (1) have been kept the same in the data and in the theoretical calculations. Modifying these definitions to account for all jets in the event changes the ratio of the cross sections by less than 10%.

Finally, the $\Delta\eta > 2$ requirement was changed to $\Delta\eta > 1$, and the analysis was repeated. For $\Delta\eta > 1$, Eq. (1) yields $x_1 \cdot x_2 > 0.005$, which results in a selection of fifteen unbiased (x_1, x_2) bins. The mean pseudorapidity interval in the selected bins is equal to 4.2 at 1800 GeV and 1.9 at 630 GeV. The average ratio of the 1800 and 630 GeV cross sections in the selected bins was measured to be $1.8 \pm 0.1(\text{stat}) \pm 0.1(\text{uncorrelated syst})$. The results are shown in Fig. 1 as a function of the mean pseudorapidity interval at $\sqrt{s} = 630$ GeV. In the case of the $\Delta\eta > 1$ requirement, the observed ratio is once again larger than the exact LO and HERWIG predictions. It is interesting, however, that HERWIG exhibits the same qualitative behavior as the data in that the ratio of cross sections decreases as the $\Delta\eta$ requirement is relaxed, whereas the exact LO

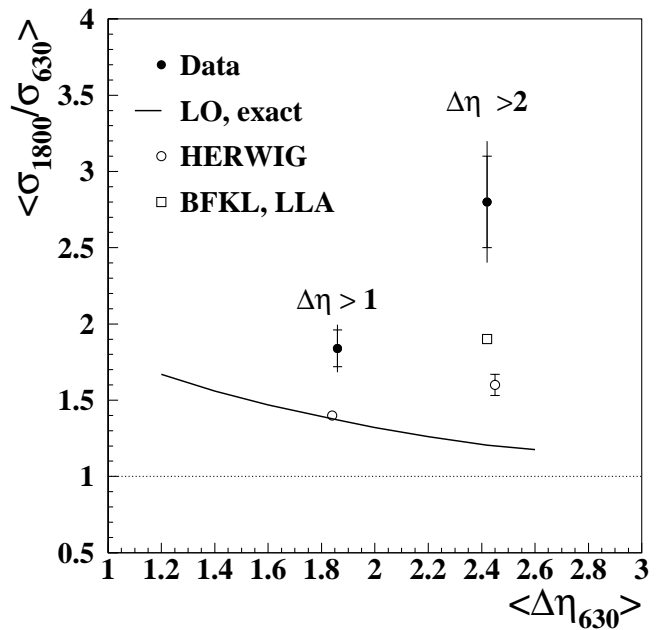


FIG. 1. The ratio of the dijet cross sections at $\sqrt{s} = 1800$ and 630 GeV for $\Delta\eta > 1$ and $\Delta\eta > 2$. The minimum jet E_T is 20 GeV. The inner error bars on the data points represent statistical uncertainties; the outer bars represent statistical and uncorrelated systematic uncertainties added in quadrature. The error bars on the HERWIG predictions represent statistical uncertainties. The LO and BFKL predictions are analytical calculations.

calculation predicts a very different trend. (A BFKL prediction is not shown for the case of $\Delta\eta > 1$ since the pseudorapidity interval is not sufficiently large for the formalism to be meaningful.)

In conclusion, we have measured the dijet cross section for large pseudorapidity intervals at $\sqrt{s} = 1800$ and 630 GeV, and the ratio of the cross sections for the same values of x_1 , x_2 , and Q^2 at the two energies. The latter corresponds to the ratio of the partonic cross sections for different values of $\Delta\eta$. The measured partonic cross section increases strongly with $\Delta\eta$, more strongly than expected on the basis of any current prediction.

We appreciate the many fruitful discussions with A. Mueller, L. Orr, and J. Stirling. We thank the staffs at Fermilab and at collaborating institutions for contributions to this work, and acknowledge support from the Department of Energy and National Science Foundation (U.S.A.), Commissariat à l'Énergie Atomique and CNRS/Institut National de Physique Nucléaire et de Physique des Particules (France), Ministry for Science and Technology and Ministry for Atomic Energy (Russia), CAPES and CNPq (Brazil), Departments of Atomic Energy and Science and Education (India), Colciencias (Colombia), CONACyT (Mexico), Ministry of Education and KOSEF (Korea), CONICET and UBACyT (Argentina), A. P. Sloan Foundation, and the Humboldt Foundation.

[1] L. N. Lipatov, *Sov. J. Nucl. Phys.* **23**, 338 (1976); E. A. Kuraev, L. N. Lipatov, and V. S. Fadin, *Sov. Phys. JETP* **44**,

- 443 (1976); *Sov. Phys. JETP* **45**, 199 (1977); Y. Y. Balitsky and L. N. Lipatov, *Sov. J. Nucl. Phys.* **28**, 822 (1978).
- [2] H1 Collaboration, S. Aid *et al.*, *Phys. Lett. B* **356**, 118 (1995); H1 Collaboration, C. Adloff *et al.*, *Nucl. Phys. B* **538**, 3 (1999); H1 Collaboration, C. Adloff *et al.*, *Phys. Lett. B* **462**, 440 (1999); ZEUS Collaboration, J. Breitweg *et al.*, *Eur. Phys. J.* **C6**, 239 (1999); ZEUS Collaboration, J. Breitweg *et al.*, *Phys. Lett. B* **474**, 223 (2000).
- [3] D0 Collaboration, B. Abbott *et al.*, *Phys. Rev. Lett.* **77**, 595 (1996).
- [4] Y. L. Dokshitzer, in *Proceedings of the 1997 International Europhysics Conference on High Energy Physics, Jerusalem, Israel, 1997* (Springer, New York, 1999), p. 47.
- [5] A. H. Mueller and H. Navelet, *Nucl. Phys.* **B282**, 727 (1987).
- [6] D0 Collaboration, S. Abachi *et al.*, *Nucl. Instrum. Methods Phys. Res., Sect. A* **338**, 185 (1994).
- [7] J. Bantly *et al.*, Report No. Fermilab-TM-1995, 1997; J. Krane, J. Bantly, and D. Owen, Report No. Fermilab-TM-2000, 1997.
- [8] B. Abbott *et al.*, Report No. Fermilab-Pub-97/242-E, 1997.
- [9] D0 Collaboration, B. Abbott *et al.*, *Nucl. Instrum. Methods Phys. Res., Sect. A* **424**, 352 (1999).
- [10] A. Goussiou, Report No. Fermilab-Pub-99/264-E, 1999.
- [11] G. Marchesini *et al.*, *Comput. Phys. Commun.* **67**, 465 (1992). We used v5.9.
- [12] H. L. Lai *et al.*, *Phys. Rev. D* **55**, 1280 (1997).
- [13] F. E. Paige *et al.*, Report No. BNL-HET-98-39, 1998.
- [14] L. H. Orr and W. J. Stirling, *Phys. Lett. B* **429**, 135 (1998).
- [15] V. S. Fadin and L. N. Lipatov, *Phys. Lett. B* **429**, 127 (1998); G. Camici and M. Ciafaloni, *Phys. Lett. B* **430**, 349 (1998).